

CO₂ conversion by reverse water gas shift catalysis: Comparison of catalysts, mechanisms and their consequences for CO₂ conversion to liquid fuels

Yolanda A. Daza and John N. Kuhn*
University of South Florida. Tampa, FL 33620

* To whom correspondence should be addressed (jnkuhn@usf.edu; telephone 001(813) 974-6498; fax n/a; Department of Chemical & Biomedical Engineering, University of South Florida, Tampa FL 33620)

Abstract

Current society is inherently based on liquid hydrocarbon fuel economies and seems to be so for the foreseeable future. Due to the low rates (photocatalysis) and high capital investments (solar-thermo-chemical cycles) of competing technologies, reverse water-gas shift (rWGS) catalysis appears as the prominent technology for converting CO₂ to CO, which can then be converted via CO hydrogenation to a liquid fuel of choice (diesel, gasoline, alcohols, etc.). This approach has the advantage of high rates, selectivity, and technological readiness, but requires renewable hydrogen generation from direct (photocatalysis) or indirect (electricity and electrolysis). The goal of this review is to examine the literature on rWGS catalyst types, catalyst mechanisms, and their implication towards their use as an operation in futuristic CO₂ conversion processes.

Keywords: carbon dioxide conversion, carbon capture and utilization, CCU, reverse water gas shift reaction, rWGS, reverse water gas shift chemical looping, rWGS-CL, CO formation, carbon monoxide.

1. Introduction

1a. CO₂ availability and current utilization

The global carbon dioxide atmospheric concentration recently reached the 400 ppm threshold, putting the world at 1.5 °C above the average temperature prior to the industrial revolution. In 2013, 32.19 giga tonnes (Gt) of CO₂ were emitted to the atmosphere [1], and emissions are expected to increase to 45 Gt/year by 2040. Approximately 22% and 33% of the yearly anthropogenic emissions are respectively absorbed into the oceans and plants, in the natural photosynthesis cycle, with the remaining 45% contributing to the increasing atmospheric concentrations [2]. An issue with oceanic CO₂ adsorption is that the gas does not absorb evenly, but rather 40% of absorption happens in the Southern Ocean [3]. By 2030, the acidification of this Ocean would likely have palpable consequences on organisms living there that could potentially affect the food web of the area [4]. The rapidly increasing atmospheric CO₂ concentration and the threat it poses upon the environment has led to increased efforts to reduce or minimize CO₂ atmospheric emissions. Amongst the most widely used approaches is Carbon Capture and Storage (CCS), more commonly called sequestration. According to the Global CCS Institute, sequestration is at a current estimated large projects (> 0.8 Mt -mega tonnes- for coal-based power plant or > 0.4 Mt for other industrial facilities) capacity of 81.5 Mt CO₂/year [5], but currently operational projects have a 28.4 Mt sequestration capacity [6]. Furthermore, current CO₂ utilizations for

industrial processes such as urea and salicylic acid synthesis (Figure 1), etc. does not exceed 120 Mt/year [7, 8]. Production of CO₂ is more than 150 times higher than its current use and potential sequestration capability (Table 1, current methods). Due to its large scale, long-term planning of a combination of methods and technologies at all levels of society, from industry to individual households, should be used if we are to significantly reduce CO₂ emissions or manufacture it into fuels and chemicals [5, 7].

Recently, a variety of technologies for repurposing the vastly abundant carbon dioxide into high value chemicals have emerged. To fulfill the ultimate resolution of environmental remediation, these technologies should be renewable, and the overall process needs to be carbon neutral or negative. Considering the limited sequestration capacity and costs of CO₂ transportation and storage (~\$ 16.5/tonne CO₂ [9]), developing technologies for Carbon Capture and Utilization (CCU) may make more sense than simply sequestering CO₂. But the stability of the molecule is another challenge to overcome. CO₂ is a very stable form of carbon, making its transformation very energy intensive.

Technologies currently under research to transform CO₂ to chemicals of wide use include synthesis of polymers [7], oxalates [10], formates [11], dimethyl ether [12], ethylene and propylene [13] and an interesting recently developed technology by Job et al. [14] that recycles CO₂ onto plastics similar to polyurethane (up to 50% CO₂ by weight). But, even at the high global demand for plastics (311 Mt in 2014 [15]), we estimate that less than 0.5% of CO₂ emissions would be used even if all the plastic produced in the world was synthesized with this technology (Table 1). Similarly, if all the methanol [16] and chemicals (made from oil) [17] consumed globally were synthesized from CO₂, emissions would not decrease by more than 0.3% and 3.8%, respectively. The comparisons of these values vividly capture the challenge of scale. Still, the key factors of utilization remain an issue: (i) the need for concentrated CO₂ [18, 19] and (ii) proven technologies for conversion that can match the scale of CO₂ production, and produce chemicals of significantly high demand [18-21].

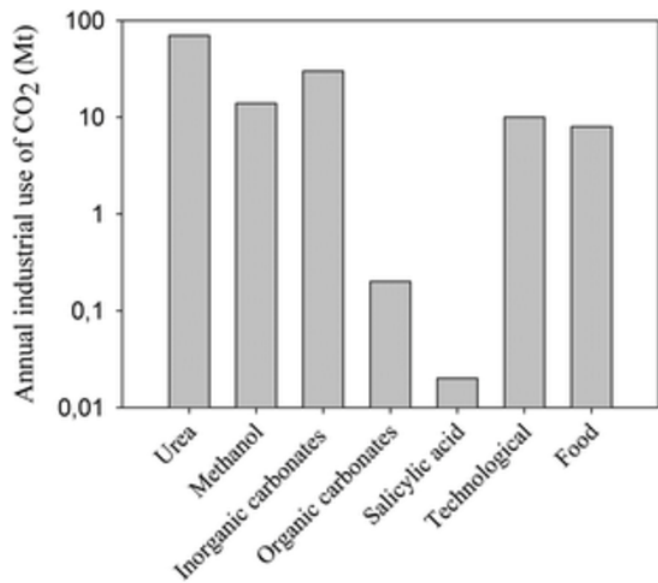


Figure 1. CO₂ use in industry. Vertical axis is on logarithmic scale. Reproduced with permission

Table 1. Potential for reduction of total emissions and atmospheric influx of CO₂ using current methods and potential end products for CO₂ conversion.

	Technique	Capacity of CO ₂ reduction (Mega tonne CO ₂ /year)	Reduction of total emissions ^a	Reduction of atmospheric CO ₂ influx ^b
Current methods	Sequestration	81.5 [5]	0.25%	0.56%
	Fine chemicals synthesis	120 [8]	0.37%	0.83%
Potential uses	Plastics	155.5 ^c	0.48%	1.07%
	Methanol	89.4 [22]	0.28% ^d	0.62%
	Oil derived chemicals	1200 [17]	3.73%	8.28%
	Gasoline	5364.6 ^e	16.67%	37.03%

^a Calculated using 2013 total emissions as 32.19 Giga tonnes/year [1]. ^b Calculated using 14.46 Giga tonnes CO₂/year absorbed by the atmosphere (45% [2] of total 2013 emissions). ^c Estimated from the technology of Job et al. [14] and plastics global demand from reference [15]. ^d In accordance with reference [16]. ^e Assuming all gasoline as C₈H₁₈ with a global demand of 94.83 million barrels/day [23] and a gallon yield of 45% v/v gasoline [24].

1b. Need for energy-dense transportation fuels

In a worldwide effort to increase environmental friendliness, the use of alternative renewable technologies (solar, wind, geothermal, nuclear, hydro...) have been steadily increasing, and have evolved from representing 2.8% of the world energy production in 1973 to 8.4% in 2013 [1]. The limitation, is that these renewable energy sources are mostly used to make electricity, and, in 2013, electricity only represented 18.0% of the global energy consumption [1]. Renewables went from representing 32.0% of all the electricity generated in 2011 [25], to 32.6% in 2013 [1]. Unfortunately, due to intermittent supply, until new methods for efficiently storing energy generated by alternate renewable sources are developed, energy dense hydrocarbon fuels, currently produced primarily from oil, will still be necessary. Hydrocarbons store substantial chemical energy, which is not possible through various transient processes until batteries, or other replacement technologies become viable.

Oil represents about 40% of world energy consumption, and in 2013, 63.8% of all oil products were used to make transportation fuels [1]. The amount of oil products that were used to make transportation fuels increased by 44.48 Mtoe (million tonnes of oil equivalent) from 2012 [26] to 2013 [1]. The demand for fuels is at least 100 times larger than chemicals [27]. Thus, only liquid fuel demand (Table 1, Gasoline as example) rivals the scale of CO₂ production [19, 28, 29]. In other words, CO₂ emissions will continue to outweigh CO₂ consumption unless hydrocarbon transportation fuels are produced from CO₂ (closed cycle) or they are no longer required. So far, no other type of energy storage vehicle has been able to outrank the practicality of liquid fuels, making energy dense fuels still necessary [30, 31]. In addition, a world-wide infrastructure for the delivery of liquid hydrocarbon fuels already exists. This avoids a major issue of the H₂ economy.

1c. Cost estimations for CO₂ conversion processes

The need for renewable hydrogen poses a crucial problem for using the carbon of CO₂ as the backbone of futuristic fuels [32-37]. With a minimum levelised cost of renewable electricity (produced by solar towers) of 0.17 USD/kWh [38], the cost of H₂ could be estimated at ~ 10 USD/kg H₂ [39] (as opposed to ~1.6 USD/Kg H₂ if electricity was not renewable [40]). This means that, if renewable H₂ was used to make one GGE of methanol, its selling price would increase by at least 4.43 USD/GGE. More recently, Kim et al. compared the cost of producing methanol with CO₂ splitting and different methods for obtaining H₂, one from WGS (using water and CO obtained from CO₂ splitting) [41] and through H₂O thermochemical splitting to H₂ [42]. They determined that thermochemical splitting of H₂O to obtain H₂ would allow for a minimal selling point of methanol at 6.73 USD/GGE [42] vs. using WGS which would produce methanol at a minimum selling point of 7.10 USD/GGE [41]. Based on these back-of-the-envelope calculations, we estimate that production of renewable H₂ would contribute about 65% (4.43 USD/GGE *100/ 6.73 USD/GGE) of the total methanol cost. It becomes evident that renewable H₂ synthesis is still a technology in development [43].

1d. Green technologies for CO₂ conversion to fuels with large demand

The technologies with the highest readiness level that are focused on converting CO₂ to synthetic fuels or their precursors (i.e. CO) are: i) rWGS reaction, ii) syngas synthesis from methane dry reforming (DR) and iii) direct hydrogenation of CO₂.

Approximately, 35 Mega tonnes of CH₄ per year are emitted to the atmosphere from landfills [44]. If instead, this gas was trapped, it could be reacted with CO₂ in a 1:1 feed to produce syngas through dry reforming. Even though methane is produced at a much lower scale than CO₂ emissions, its use could be advantageous because it is naturally being produced. Nonetheless, DR is an endothermic reaction [16], favored at high temperatures (> 900 °C), at which catalysts sinter and coke [30]. Often, landfill gas contains high level of sulfur gases which cause catalyst deactivations [16]. Low temperature DR has been reported (430–470 °C) with no coking, but using an assembly of noble and transition metal catalysts combined with metal oxides (Pt–Ni–Mg/ceria–zirconia catalysts [45]) which have yet not been studied for sulfur poisoning.

Direct CO₂ hydrogenation is more thermodynamically favored than rWGS. Therefore, it was considered promising for industrialized methanol synthesis [46] and has been demonstrated on a pilot scale in Iceland by George Olah and Surya Prakash. However, the CAMERE (Carbon Dioxide Hydrogenation to form Methanol via Reverse-Water-Gas-Shift Reaction) process revealed 20% higher methanol yields when CO₂ is converted to CO (through rWGS), and CO to methanol, rather than directly hydrogenating CO₂ [33].

Other methods, such as photo-electro-chemical reduction, are currently not a viable way to convert massive CO₂ amounts, because its low rates which would highly difficult a process scale up that can match CO₂ production rates [47, 48]. Similarly, if using biomass, atmospheric CO₂ concentrations can only be lowered if such biomass is converted to fuels, otherwise it is not a long-term storage of the CO₂ [49, 50]. Conversion of CO₂ to biofuels using biomass that does not

compete with food and does not require land, would likely involve the use of microalgae. But the costs of cultivating and maintaining these systems would have to substantially reduce before it becomes feasible [49-51]. An upcoming technology, thermochemical CO₂ splitting, also referred to as thermochemical cycles (TCs), has the advantage of not requiring an additional reactant (other than CO₂). In this technology, CO₂ is reduced to CO on the oxygen vacancies of a metal oxide with high oxygen mobility. TCs for CO₂ splitting have been demonstrated on several oxides [52-57], but they usually require at least 1000°C for the formation of oxygen vacancies or several hours to be reduced at lower temperatures. On these oxygen vacant materials, the conversion of carbon dioxide to carbon monoxide has been achieved at ~900 °C [52, 54-56]. The high operational temperatures would require specialized gear, and additional equipment (such as solar concentrators) that can generate the required heat input.

The rWGS is an endothermic reaction, favored at high temperatures [36]. The most commonly studied catalysts are copper based [58-61], or supported ceria [62-64], potentially less expensive than those used in DR. Its biggest advantage is the formation of CO, which can be used as a building block for a variety of important chemicals, such as hydrocarbons in Fischer-Tropsch synthesis, fine chemicals synthesis or the purification of nickel. The rWGS is suspected to be a key step in selective methanation of CO₂ [65] and to occur in FT reactors with high CO₂ feeds [29, 66]. It becomes evident that rWGS is a key reaction that should be considered and fully understood.

1e. Rationale for rWGS catalysis over competing technologies

The rWGS reaction was first observed by Carl Bosch and Wilhelm Wild in 1914, when they attempted (and halfway succeeded) to produce H₂ from steam and carbon monoxide on an iron oxide catalyst [67]. Currently, it is important in the synthesis of methanol [19] and in fixing syngas' H₂/CO ratio for various applications.

Mallapragada et al. [68] compared different routes to transform CO₂ into liquid fuels (biomass gasification, rWGS, algae-derived oils and direct photosynthesis) using solar assisted processes and H₂ provided by electrolysis. Amongst the investigated methods, conversion of CO₂ to CO by reverse water gas shift reaction followed by CO conversion to fuels with FTS had the highest current and estimated potential efficiency when CO₂ is captured from a flue gas or from the atmosphere [68]. Furthermore, converting CO₂ to CO gives an added versatility in the products that can be obtained from CO transformation [17]. The rWGS is also of great interest to be used in space exploration due high (~95%) atmospheric CO₂ concentration on Mars, and availability of H₂ as a byproduct of oxygen generation [69, 70]. Therefore, rWGS is a promising reaction, whose products have a wide variety of potential end uses.

The rWGS shift reaction is advantageous because of its technical feasibility compared to alternative technologies. However, as will be described in section 1f, many of the alternative technologies hold much promise if future research advances overcome significant existing challenges. In addition, with the CO₂ problem being one of such massive scale and with local resources (e.g., solar insolation, available land and water, etc.) varying significantly, a multi-pronged approach is most probable, with the rWGS reaction using renewable hydrogen being one route.

1f. Goals and limitations of this review

For the arguments already described in this review, conversion of carbon dioxide is an increasingly interesting topic for which many critical advances are needed to make substantial contributions. The readers are directed elsewhere for superb reviews on chemical conversion to a variety of organic products [13, 71-76], solar-thermal-chemical cycling [77-79], dry reforming [80-82] and other reactions with methane [83] and photo-electro-catalytic conversion [84-88]. Excellent overviews [89, 90] and reviews on CO₂ separation [91-93] (including from air [94]) and the forward water gas shift [95] are also already available and may be of interest. Comparatively, there is very little summarized for the rWGS even though it is a promising reaction as part of a CO₂ conversion system and likely the closest to implementation. Thus, the primary goal of this review is to summarize literature findings for the rWGS reaction, with an emphasis on a discussion of comparing catalyst types, rates, mechanisms, and intensification strategies. Although the forward reaction has been examined in much more depth, this review primarily focuses on literature using CO₂ and H₂ as the feed, so studies on H₂ purification via the forward WGS are not included.

In addition, as a secondary goal, the scope of CO₂ conversion and the authors' vision for this challenge of scale has been justified in the introduction. The authors envision a society where transportation fuels and chemicals are produced from various CO₂ purification and conversion strategies while solar, wind, geothermal, etc are employed for renewable electricity. Since CO₂ capture continues to be realized at various degrees, conversion strategies can operate under the assumption that CO₂ will be available from flue gas or atmospheric separations (taking a concentration cost but minimizing contaminant issues), which makes the conversion processes a gate-to-grave type comparison. The advantages of the rWGS approach to the conversion are that:

- A variety of renewable electricity forms exists with various advantages occurring locally. The rWGS reaction can be implemented with any of them to contribute to a closed carbon loop.
- Hydrogen from electrolysis requires much lower capital costs than using solar-thermal-heating to magnify the low intensity solar flux to practical levels.
- The rWGS reaction produces CO which is a very flexible chemical intermediate. Alternatively, the hydrocarbon product from photocatalysis is primarily methane which still requires processing for use.
- Any process that generates CO still requires ~ 2 moles H₂:1 mol CO to achieve a value-added fuel or chemical. The additional 1 mol H₂ for convert CO₂ to CO is just increasing the amount required from H₂ generation processes by 50%, not substantiating their existence in the overall process.
- Although not common, the rWGS may be useful in applications where H₂ is readily available such as space exploration where electrolysis is primarily used for synthetic air production.

For these reasons and the readiness of the rWGS processes, its application in future CO₂ conversion strategies seems likely. To reiterate, other strategies such as a closed loop of biomass conversion are also attractive but it is unlikely that one approach would be advantageous globally. With the justification provided above, energy dense liquid hydrocarbon fuels will continue to be a transportation fuel of choice. But transportation fuels far exceed other chemicals for contributing to the scale of the CO₂ problem, therefore rWGS with methanol synthesis or FTS and biomass

conversion to fuels are needed to rise to the challenge of achieving a closed carbon loop. In addition, with either synthetic (chemical) or natural (biological) CO₂ separation from air, and conversion to plastics as a secondary, albeit smaller scale, route of conversion, it may be possible to decrease atmospheric CO₂ concentrations provided that electricity is primarily from renewable sources.

2. Thermodynamic considerations

The rWGS (eq. 1) is equilibrium limited, and favored at high temperatures due to the endothermic nature of the reaction.



Additional side reactions include:

Methanation



and the Sabatier reaction



Thermodynamic evaluations at atmospheric pressure, show that CO₂ conversion in rWGS is enhanced when excess H₂ is flowed [35] and equilibrium conversion increases with temperature [35, 96] (Figure 2). Products separation can shift the equilibrium towards the products [27]. Whitlow and Parrish from Florida Institute of Technology and NASA, respectively [69], built a rWGS demonstration reactor without a catalyst in the system. They incorporated a membrane reactor to separate the products and achieved close to 100% CO₂ conversion (~ 5 times the equilibrium conversion). When the H₂/CO₂ flow is 0.5, CO₂ conversion is 1/4 lower than the equilibrium conversion with a 1/1 flow at the same temperature, but when the flow ratio is 2, the conversion is enhanced by 50%. Optimum operating conditions were 310 kPa and 400 °C. Medium-pressures were used in the study and it was found that small variations on the pressure (131 to 310 kPa) have no effect on the conversion [69].

In a PNNL report, VanderWiel et al. [70] studied the rWGS and Sabatier reaction for CO₂ conversion. rWGS needs to be operated at very low residence times (5 to 64 ms) to achieve the highest CO selectivity (higher than equilibrium) but a methane side product was observed in the rWGS experiments. At residence times of 32 ms, CO selectivity reaches equilibrium at ~ 550 °C. No CO₂ conversion was observed below 300 °C. Further ways to shift reaction equilibrium or increasing reaction rates involves the use of electricity. Applying an overpotential to the Pd-YSZ electrode increased the rate of the reaction [97], while applying 3.0 mA to the 1 wt%Pt/10 mol%La-ZrO₂ catalyst was equivalent to increasing the temperature by 100 K [35]. In both studies, CO was the only carbonaceous product.

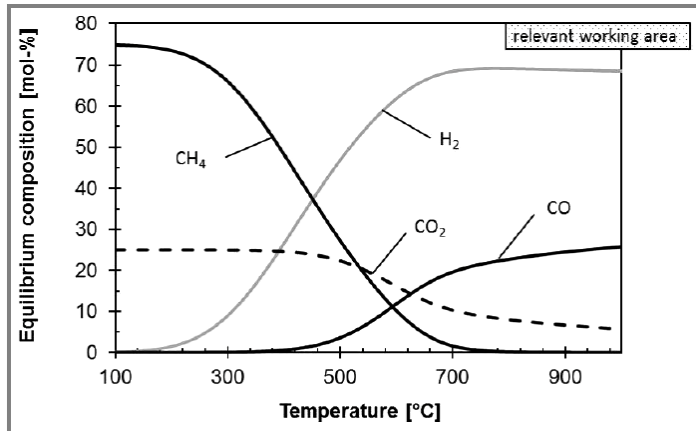


Figure 2. Influence of temperature on the thermodynamic equilibrium of the rWGS at 1 bar and $H_2/CO_2 = 3/1$ molar. Reproduced with permission from John Wiley and Sons (from [17]).

3. Catalyst types

3a. Supported metal catalysts

The rWGS studies of supported metal catalysts consist primarily of Cu, Pt, and Rh immobilized on a variety supports. Studies on these metals are first highlighted. Then, screening studies of a wide variety of metals are discussed. Finally, support effects are reviewed.

3a-I. Copper

The use of Cu for rWGS devises two major advantages, i) it has been shown to perform rWGS at low temperatures (~ 165 °C) [98], and ii) little or no methane is formed as a side product [99-101]. But without hydrogen, CO_2 dissociation is highly unfavorable on clean Cu surfaces [102-105], which directly translates to the need of high H_2/CO_2 feed ratios to achieve high CO_2 conversions. More insights into the hydrogen-aided activation will be discussed in the mechanisms section. Therefore, the enhancement of Cu activity has been extensively studied by incorporation of supports and/or promoters to the catalytic system.

Chen et al. have several contributions on the rWGS on Cu nanoparticles supported on different metal oxides. In their first study, they determined that supporting Cu NPs on Al_2O_3 increased the adsorption of formates, which they proposed as the reaction intermediates [101]. In their other contributions examining CO_2 hydrogenation on Cu nanoparticles [106], and Cu nanoparticles supported on SiO_2 [107], they also concluded that i) the rWGS mechanism goes through a formate intermediate [106, 107], ii) the CO_2 and CO adsorption sites for the forward and reverse mechanisms are independent [106], and iii) high Cu dispersion on SiO_2 enhances CO_2 conversion [61]. Ginés et al. [59] also observed that high Cu dispersion was a characteristic of the catalyst with highest activity on a Cu/ZnO/ Al_2O_3 system.

Chen et al. also studied promoting the reaction with potassium [100] and iron [60, 96] in the Cu/ SiO_2 system. In general, a promoter addition enhanced catalytic activity, but both metals had slight different effects. Fe prevented Cu NPs sintering, significantly enhancing the stability and

activity of the catalyst [60, 96], whereas K increased the surface active sites that can adsorb and decompose formates, enhancing the catalytic activity of the system [100].

3a-II. Platinum

At low temperatures (100 to 300 °C), CO₂ is converted to CO on the interface between Pt and CeO₂ after H₂ pre-treatment, but CO formation was not observed on CeO₂ or Pt alone [108]. Supported platinum (on La-ZrO₂) showed increased CO₂ conversion when compared to supported iron and copper, but lower selectivity towards CO, as demonstrated on electrically promoted (E-rWGS) experiments [35].

Meunier's group has dominated most of rWGS studies on Pt supported samples. The group observed different surface reactive compounds in a 2% Pt/ CeO₂ catalyst depending on the reaction conditions [109]. When the reaction intermediates were allowed to accumulate under vacuum, formates were observed as the most reactive, but under steady state conditions, the most reactive surface compounds were carbonates and carbonyls. These results shed some light on the dispute of carbonates or formates as the main reaction intermediates. High temperature DRIFT and steady-state isotopic transient kinetic analysis (SSITKA) on 2% Pt/CeO₂ confirmed that the main reaction intermediates were carbonates and not formates, although CO formation from formates could also occur in minority [110]. Observed carbonates could be mono or bi-dentate [108]. On a solid-liquid interface, rWGS was found to occur on a Pt/Al₂O₃ system by a redox mechanism, where the O adatom (formed from CO₂ dissociation), can refill an Al₂O₃ surface vacancy or recombine with adsorbed H [111].

The effect of adsorbed reactants and products has also been investigated in Pt systems. Jacobs and Davis [112] studied the effect of H₂O and H₂ adsorption on 1% Pt/CeO₂ during rWGS and observed different spectator species formed under different conditions, suggesting that the forward and backwards WGS mechanism could be different. Even though Pt/SiO₂ systems have achieved higher conversion than Cu/SiO₂ at 500 °C [61], poisoning of Pt by CO has been observed in 2% Pt/ CeO₂ [113], and on Pt and Ru/Pt alloy electrodes on PEMFCs [114]. Bimetallic Co-Pt particles were tested for rWGS but it was found that Pt migrates to the surface, almost inhibiting any Co effect. The selectivity towards CO is highly increased, but there was no mention of CO₂ conversion [115].

3a-III. Rhodium

Rh is widely used in homogeneous CO₂ hydrogenation, mostly in amine solutions [116]. However, for Rh deposited on different supports (MgO, Nb₂O₅, ZrO₂ and TiO₂), the combined selectivity towards methane and methanol added to more than 80% at temperatures between 100 and 300 °C and H₂/CO₂ =3 feed ratios [117]. Matsubu et al. [118] determined that the selectivity of CO vs. CH₄ on Rh/TiO₂ increased at low Rh loadings at 200 °C and low H₂/CO₂ feeds. When Rh is deposited in small loadings, it is dispersed on the surface, forming isolated Rh sites where CO₂ conversion to CO is preferred. At large loadings, Rh forms NPs, which hydrogenate CO₂ to CH₄. Similarly, high availability of H adatoms can also favor CH₄ formation.

For Rh/SiO₂, increasing the surface hydroxyl groups surrounding Rh particles on the catalyst surface increases CO₂ conversion and selectivity towards CO because it leads to formation of Rh carbonyl clusters, whereas less hydroxyl groups form hydride species on the Rh surface, that can further hydrogenate CO to methane [119]. Li was added to an Rh ion-exchanged zeolite (Li/RhY) [120] and the selectivity towards CO (vs. CH₄) was found to increase with amount of Li promoter, going from 0.3% at no Li, to 86.6% at 10:1 Li:Rh atomic ratio, but CO₂ conversion was decreased to half with Li addition.

3a-IV. Other transition metals and bimetallic particles or systems

Electrically promoted rWGS was performed on M/ La-ZrO₂ (M= Pt, Pd, Ni, Fe, Cu) at 150 °C. CO₂ conversion was the same for Ni, Fe and Cu supported on La-ZrO₂, but 100% CO selectivity was achieved on Fe and Cu, while only slightly lower conversion (96.5%) was achieved on Ni [35]. DFT studies demonstrated that chemisorption energies of CO₂ are increased from early to late transition metals (Fe to Cu) (100) surfaces. But due to very strong and weak interactions with Fe [103, 105] and Cu [102-105], respectively, Co and Ni were deemed more favorable [103]. Experimentally, increasing Ni content in a Cu-Ni system supported on γ -Al₂O₃, had no effect on CO₂ conversion but decreased CO selectivity [121].

Lu et al. [122] observed that, at low NiO loadings (< 3%) on CeO₂, the particles were monodisperse on the ceria matrix and lead to 100% selectivity towards CO from 400 to 750 °C, while higher loadings lead to aggregation and lower CO selectivity below 650 °C. Sun et al. [123] observed similar results on Ni/Ce-ZrO₂, increasing Ni loading decreased CO selectivity and CO₂ conversion, with the exception of 1% and 3% Ni, which exhibited similar behaviors. In conclusion, including Zr appears to lower CO selectivity and CO₂ conversion [122, 123].

Wang et al. [64, 124, 125] demonstrated that different methods for supporting Ni on CeO₂ affect CO₂ conversion and CO selectivity, where the oxygen vacancies and highly dispersed surface Ni species were found to have the leading role in the reaction activity. The highest rWGS activity was observed on the catalyst synthesized by impregnation because the Ni is deposited as NiO, which favors CO formation (as opposed to methane) [64]. The 1% Ni/CeO₂-impregnation catalyst achieved up to 45% conversion and 100% selectivity towards CO in a 1:1 H₂/CO₂ flow at 750 °C [64]. Comparing this result to other studies, it appears that increasing Ni loading increases the activity of the catalyst. 2% Ni/CeO₂ showed stability for over 9 h and constant CO yield (35% in a 1:1 H₂/CO₂ flow) at 600 °C, and 45% CO selectivity at 750 °C [124], whereas 3% Ni/(Ce-Zr)O₂, achieved 50% CO₂ conversion and 100% CO selectivity at 750 °C (in a 1:1 H₂/CO₂ flow) for 80 h [123]. Supporting nickel on SBA-15 did not have a significant impact on the catalyst activity [126], but incorporation of Cu in a bimetallic Cu-Ni/SBA-15 system improved CO₂ conversion and CO selectivity [127], as expected.

Ko et al. [128] also performed CO₂ dissociation DFT studies on different bimetallic alloy surfaces and determined that Fe alone and Fe-containing bimetallic particles would be the most favored to dissociate CO₂ to CO and O. Unsupported Fe-oxide NPs (10 to 20 nm) were tested for 19 h showing high stability and medium CO₂ conversion (~30%). The stability of the sample could have come from migration of C and O into the catalyst bulk forming iron oxide and iron carbide, which likely kept the NPs on the surface from agglomerating [129]. Kharaji et al. [130] determined

that the supported bimetallic Mo-Fe/ γ -Al₂O₃ system, increased CO formation rates, CO₂ conversion and CO selectivity when compared to the monometallic versions of the catalyst (Fe/ γ -Al₂O₃ or Mo/ γ -Al₂O₃) [130]. The leading role of the conversion was attributed to Fe while Mo enhanced the stability of iron by increasing the electron deficient state of Fe-species, enhancing catalytic activity [130]. Addition of Ni to the Mo/Al₂O₃ system also showed increased activity [131]. Incorporation of Fe has also increased CO selectivity in a Rh/TiO₂ system, but highly decreasing CO₂ conversion [132]. Porosoff et al. [133] showed that adding Co into Mo₂C enhances CO₂ conversion and CO selectivity at 300 °C when compared to Pt-Co and Pd-Ni bimetallic NPs supported on CeO₂. But Ni/Mo₂C and Cu/Mo₂C have shown higher CO₂ conversion and CO selectivity than Co/Mo₂C catalysts [134].

In₂O₃ has been found to inhibit CO production [135], but bimetallic In-Pd NPs supported onto SiO₂ have achieved 100% CO selectivity on the rWGS [136], although with lower activities than Pd/SiO₂. DFT suggested that the bimetallic Pd-In NPs had a weaker CO adsorption than Pd NPs, which suppresses the possibility of further hydrogenating CO to CH₄ on the bimetallic system [136].

3a-V. Support effects

CO formation rates on Rh supported on TiO₂ increased two orders of magnitude when compared to MgO, Nb₂O₅ and ZrO₂ as supports [117]. rWGS studies on a Pt/TiO₂ system demonstrated that TiO₂ was an active component in the reaction, likely H₂ reduction led to the formation of Pt-Ov-Ti³⁺ sites (Ov = oxygen vacancies) [137]. The reaction activity was inversely proportional to the reducibility and crystallite size of TiO₂ [137]. Sakurai et al. [138] compared activities in Au NPs supported on TiO₂, Al₂O₃, Fe₂O₃ and ZnO at two system pressures (P = 0.1 and 5 MPa). TiO₂ exhibited the highest activity at all reaction conditions (T = -123.15 to 126.85 °C). On this sample, CO selectivity was increased at the lowest pressure tested. Al₂O₃ and Fe₂O₃ also exhibited high activity at 0.1 MPa but it significantly decreased at 5 MPa, while ZnO had a low activity at both system pressures [138].

Amongst Pt/TiO₂ and Pt/Al₂O₃, titania exhibited higher activity and CO selectivity [139]. Different lanthanide oxides were tested as Pd supports for the reaction and the activity order was found to be CeO₂ > PrO₂ > La₂O₃ [140]. When ceria has been incorporated into an Fe/Mn/Al₂O₃ system, CO selectivity was enhanced, but CO₂ conversion was slightly decreased [141]. Ceria is almost 100% selective towards CO at T \geq 550 °C [142], likely because at higher temperatures the oxygen mobility of the oxide increases. Oxygen vacancies of ceria have been proven to play a leading role on the Pd / CeO₂ / Al₂O₃ system, because they can re-oxidize with CO₂, while the role of Pd is of enhancing the reduction of ceria [140]. Different shapes of cerium oxide have been tested for the rWGS and it was found that the reaction in ceria is not shape sensitive [142]. Also, supporting Ni on ceria slightly enhances CO₂ conversion but significantly improves CO selectivity [142], as discussed in the previous section.

3b. Oxide catalysts

The CAMERE process uses a rWGS and a methanol synthesis reactor to convert CO₂ to methanol [33]. The first catalyst proposed on the CAMERE process consisted on Cu NPs on a

ZnO/ZrO₂/Ga₂O₃ support at 250 °C [33]. Curiously, ZnO has been shown inactive for rWGS at temperatures below 165 °C [98, 143]. A later CAMERE catalyst consisted of ZnO/Al₂O₃, which showed enhanced stability (tested for over 100 h) at temperatures above 700 °C [143]. The motivation for high temperatures was to favor the reaction thermodynamics. Cu was removed from the catalytic system likely because of low stability due to sample loss from the Cu oxides reduction [59]. ZnO was tested at 600 °C for 60 h and showed high deactivation. The ZnO/Al₂O₃ catalyst exhibits less CO₂ conversion at 600 °C but high stability for over 200 h [144], likely due to the formation of a ZnAl₂O₄ spinel [143, 144].

Theoretical CO₂ adsorption and hydrogenation studies on the (110) In₂O₃ surface suggested that In₂O₃ suppressed rWGS due to weak CO₂ adsorption [145] and has also been found to inhibit CO production [135]. Incorporation of CeO₂ to In₂O₃ increased CO₂ conversion (at 500 °C in a 1:1 H₂/CO₂ flow) from 2.5% (In₂O₃) to 20% (In₂O₃: CeO₂, 1:3 w/w ratio) by increasing oxygen mobility, the adsorption of CO₂ and generation of adsorbed bicarbonate species [62]. Similarly, incorporation of ceria to a Ga₂O₃ (Ga:Ce molar ratio of 99:1) increased CO₂ conversion by 1.3% when compared to Ga₂O₃ at the same conditions described above [63]. Both studies observed increased amounts of adsorbed bicarbonate species [62, 63], which were suspected to be promoted by enhance of oxygen mobility by ceria [62], but neither study quantified CO selectivity or yield.

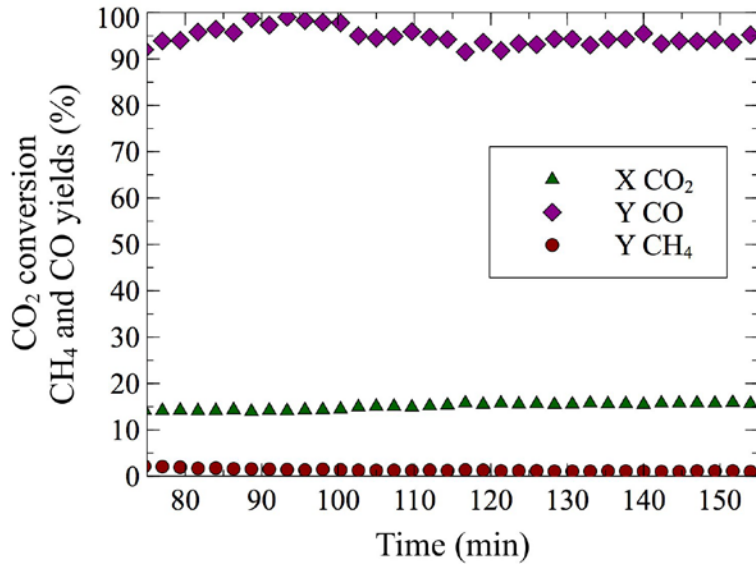


Figure 3. Reverse water gas shift reaction over 78.3mg of La_{0.75}Sr_{0.25}FeO₃ at 550 °C. Total flow 50sccm (10% H₂ 10% CO₂ v/v, He balance). Previously, catalyst was reduced for 20 min in 10% H₂/He at 550 °C.

Perovskites with La on the A site and Cu [146-148] or Co [149] on the B site have been studied for CO₂ hydrogenation to methane and methanol. CO formation was observed by Kim et al. [150] with 97% selectivity and almost 40% CO₂ conversion at 600 °C and 1 bar, on a BaZr_{0.8}Y_{0.16}Zn_{0.04}O₃ oxide. With a La_{0.75}Sr_{0.25}FeO₃ perovskite (for synthesis method see [151]), we were able to achieve a steady state conversion of 15% at 550 °C (Figure 3). The sample was reduced for 20 min at 10% H₂/He and after 20 min of flushing (100% He), the rWGS reaction (10% CO₂ / 10% H₂ / He) was performed for 90 min. The obtained rate (1.53 millimol CO/g P/min) was three orders of magnitude larger than Goguet et al. [113] and Chen et. al [101] but at higher

temperatures. rWGS on perovskites, $\text{BaZr}_{0.8}\text{Y}_{0.16}\text{Zn}_{0.04}\text{O}_3$ [150] and $\text{La}_{0.75}\text{Sr}_{0.25}\text{FeO}_3$ (this work), exhibited the added advantage of nearly 100% CO selectivity without the use of supported nanoparticles. A comparison of selectivity, conversion and different reaction conditions for multiple catalytic systems can be found on Table 2.

4. Intensified rWGS

The first attempts to achieve an intensified rWGS process emerged from combining chemical looping with DR, but substituting CH_4 by H_2 due to its higher potential as a reducing agent. In a chemical looping process, the ability of the oxygen carrier to reduce and oxidize under the desired environments in a key factor that can determine the feasibility of the process. In the rWGS process combined with chemical looping, a metal oxide is used as an oxygen carrier (Figure 4). First, H_2 is used to reduce the metal oxide. Subsequently, CO_2 serves as an oxidant, returning the metal oxide to an oxidized state while CO is formed. The main advantages of an intensified rWGS – chemical looping process (rWGS-CL) are eliminating the possibility of methanation because the $\text{H}_2/\text{H}_2\text{O}$ and CO/CO_2 flows are kept separate, and inherent product separation [151-153], which drives the equilibrium towards the products. In addition, no excess hydrogen is required because the reactions involving the metal oxide are stoichiometric.

Thermodynamic modeling and experimental screening of transition metal oxides showed that Fe-based materials had one of the best CO_2 carrying capacities while having the ability to function in the widest variety of temperatures [154, 155]. Najera et al. [154] observed signs of stability on a 40% w/w Fe-BHA (Barium Hexaaluminate) porous sample on the intensified rWGS process over 6 reaction cycles and Galvita et al. [156] used a $\text{Fe}_2\text{O}_3\text{-CeO}_2$ composite and found that adding ceria to iron oxide linearly enhanced the stability of the solid solution, but decreased the CO formation capabilities. The same group later studied different weight loadings of Fe_2O_3 on a $\text{Al}_2\text{O}_3\text{-MgO}$ system, and found that at low loadings of iron oxide (≤ 30 wt %) the oxygen storage capacity of the samples decreased, but these samples are still preferred for CO_2 conversion because of the high stability of the structure that Fe, Mg and Al form during the redox cycles [157].

The rWGS-CL process was demonstrated on $\text{La}_{(1-x)}\text{Sr}_x\text{CoO}_3$ perovskite oxides by Daza et al. [152], but amongst the studied temperatures, the H_2 reduction and CO_2 conversion happened with at least 50 °C difference, so the process was not isothermal. Reduced Fe-based spinels had been used previously for CO_2 decomposition to $\text{C}_{(s)}$ and $\text{O}_{2(g)}$ at 300 °C [158, 159]. Based on this results, the rWGS-CL process was further examined using $\text{La}_{0.75}\text{Sr}_{0.25}\text{FeO}_3$ and an isothermal process at 550 °C was achieved [151]. By substituting cobalt with iron, the reducibility of the material was significantly decreased and it did not decompose under H_2 flow. However, the process was not fully stoichiometric, because even though oxygen vacancies were being created, not all of the vacancies were re-filled. DFT suggested that the driving force for the CO_2 bond cleavage was the increased CO_2 adsorption strength at the highest vacancies extent tested. rWGS was tested on $\text{La}_{0.75}\text{Sr}_{0.25}\text{Fe}_{(1-y)}\text{Cu}_y\text{O}_3$, but doping Cu into the B site of the perovskite highly increased its reducibility and inhibited CO formation [153].

CO formation was achieved on both cobalt- and iron-based perovskites at similar reaction conditions, but the different solid state reactions the oxides underwent suggest very different reaction pathways. The high reducibility of the Co-based perovskite [152] lead to its reduction to

base La_2O_3 and metallic Co. It is likely that CO_2 then adsorbed in the basic lanthanum oxide or lanthanum-based Ruddlesden Popper phase and dissociated in the metallic cobalt, turning the metal into cobalt oxide (CoO) while yielding CO. On the iron based material, a surface redox mechanism between oxygen vacancies in the perovskite took place, where the CO_2 was adsorbed likely on a lanthanum and oxygen surface termination [160] close to an oxygen vacancy, then CO_2 can dissociate into CO and a O adatom that re-fills the said oxygen vacancy [151]. Introducing Cu into the Fe-based perovskite likely increases the stability of the perovskite in its reduced state (after forming oxygen vacancies), therefore reducing its oxygen affinity and re-oxidation capabilities, consequently the observed outcome was a suppression of CO production because CO_2 was not able to re-oxidized the reduced copper oxide [153].

Throughout the different studies with an intensified version of the conventional rWGS reaction, the highest rates were achieved with Fe-containing solid solutions. A comparison of all studies covered in this section is shown in Figure 5. Even though it has been shown before that Fe-oxides can decompose CO_2 to C(s) and O_2 [158, 159], Fe-based oxides show the highest CO formation, and almost all materials shown in Figure 5 contain a form of iron. Only one study has tested selectivity towards CO (vs. C(s)) and the process is 30 times more selective towards CO [151]. As in conventional rWGS, high temperatures enhance the intensified process for CO_2 conversion. The materials with the highest CO formation rates, were tested at high temperatures and with high loadings of iron. In addition to being performed at high temperatures and containing a high loading of iron, the Fe_2O_3 - CeO_2 mixture exhibited the highest CO formation rates likely due to the high oxygen mobility of ceria [156]. Curiously, even though Cu is widely used to catalyzed forward and reverse water gas shift, Fe works best for the intensified process.

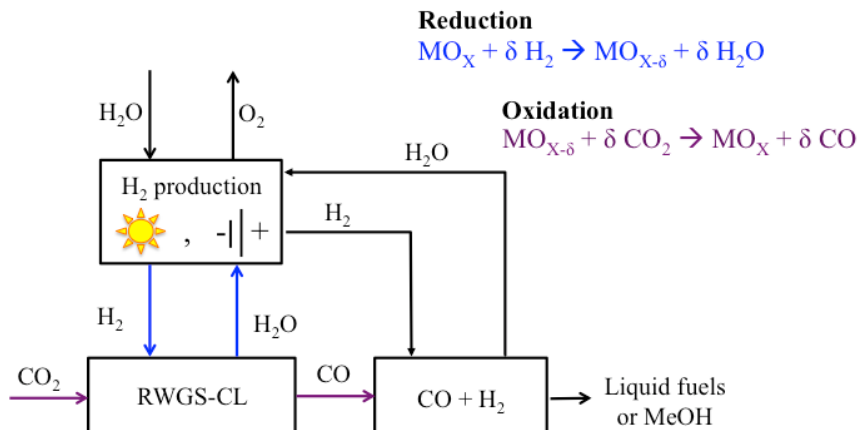


Figure 4. Pictorial representation of the intensified reverse water gas shift (rWGS-CL) process. Modified with permission from American Chemical Society (from [152]).

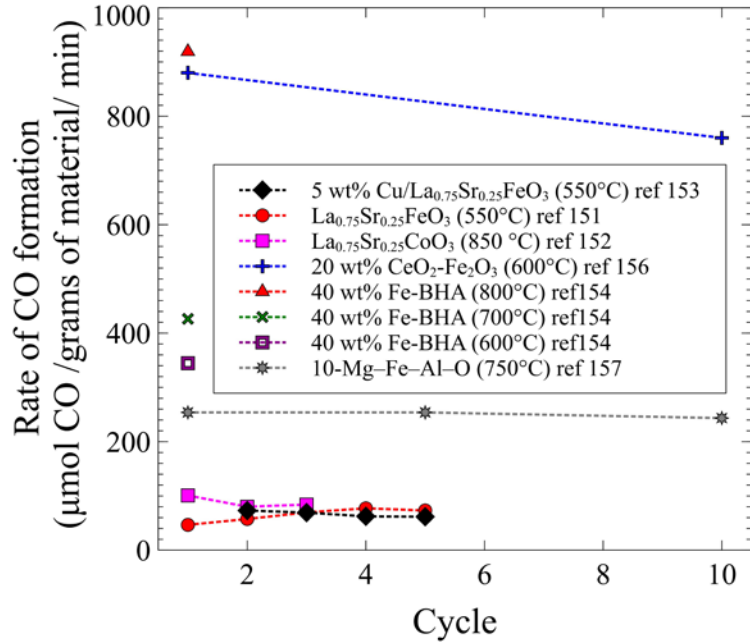


Figure 5. CO formation as a function of cycle in the intensified rWGS-CL process from references [151-154, 156, 157].

5. Mechanistic Considerations

5a. Copper surfaces and supported copper nanoparticles

Studies performed on Cu surfaces [58, 161] and supported Cu/ZnO systems [59] agreed that reaction orders (and therefore the rate limiting step) vary with reaction conditions. Kinetic studies over Cu (100) single crystals [58] and commercial Cu/ZnO/Al₂O₃ [59] demonstrated that the reaction orders with respect to PH₂ and PCO₂ change with the partial pressure of the gases.

Ernst et al. [58] and Ginés et al. [59] studied the dependence of the reaction orders for H₂ and CO₂ in the rWGS reaction. Both studies agreed that at low PCO₂/PH₂ (below 1/3 for [59] and below 1/10 for [58]), the reaction rate is highly dependent on PCO₂ (order of ~1.1 [59] and 0.6 [58] for CO₂) and independent of H₂ (0 order) [58, 59], likely due to a deconstruction of the surface, which makes it more favorable for CO₂ dissociation [58]. Whereas at intermediate pressures (PCO₂/PH₂ > 1/3 for [59] and 1/10 < PCO₂/PH₂ < 1/2 for [58]) the studies disagree. Ernst et al. state that, within the mentioned pressure interval, the rate depends strongly on PH₂ and it is independent of PCO₂ (0 order for PCO₂), whereas Ginés et al. believe that the reaction rate is dependent on both gases (order 0.3 for PCO₂ and 0.8 for H₂). At very low PH₂, the surface coverage of H₂ is lower and cannot form the favored surface [58, 59], therefore the reaction rate is highly dependent on PH₂ (2nd order for PH₂) [58]. At higher PCO₂/PH₂ ratios, the rate is again linearly dependent on CO₂ pressure [58, 161]. High coverage of H atoms adsorbed on Cu surfaces enhance CO₂ conversion, regardless of if the hydrogen is provided as molecular hydrogen (H₂) [58] or electrochemically supplied (H⁺) in solid oxide fuel cells [162, 163].

Reaction rates for the rWGS on Cu(110) and Cu(111) surfaces were comparable to Cu/ZnO except with high H₂/CO₂ partial pressures ratio. This was consistent with results that show ZnO is not

very active for rWGS [98, 143] (as mentioned in section 3b). In the high H₂/CO₂ partial pressures case, the CO₂ decomposition mechanism seems to be aided by adsorbed H adatoms, which can adsorb in the Cu/ZnO surface but not on Cu(110) and Cu(111) [161] (Figure 6).

Even though dissociation of CO₂ on the Cu atoms is considered the rate determining step [98], it is worth to mention that the probability for CO₂ dissociation on H-adsorbed Cu surfaces is two orders of magnitude larger than on clean Cu [161] surfaces. Therefore, surface modifications by H have been suspected to favor the reaction [161]. Rates have increased one order of magnitude by supplying electrochemical hydrogen (H⁺) in Cu electrodes in solid oxide fuel cells [163]. Furthermore, in UHV conditions, no CO₂ dissociation has been observed [102].

In general, addition of alkali metals may alter the catalytic system reactivity [164]. Adding K as a promoter in a Cu/SiO₂ system, increases the amount of active sites by increasing the positive charge on the catalyst surface [100], which has been found favorable for the reaction because increasing surface positive charges is less favorable for CO adsorption and its reduction to methane and other products [130] (Figure 6).

5b. Interactions of supported platinum nanoparticles with oxygen vacancies of supports

The rWGS mechanism on supported Pt/ceria systems has been highly debated. Jin et al. [108] determined that CO₂ is converted to CO on the interface between Pt and CeO₂ (Figure 7), but neither on CeO₂ or Pt alone (between 100 and 300 °C). An important observation from this study is that CO (resulting from CO₂ decomposition) is adsorbed on Pt the same way as if CO was flowed directly [108]. This suggests that the transport and/or desorption of the CO and O species (after CO₂ dissociation) is not the rate limiting step, but rather the dissociation of CO₂ itself.

Formates have been observed as the most reactive intermediate on an inert atmosphere [109] and when H₂O is included in the rWGS feed [112]. Supplying electrochemical hydrogen (H⁺) in Pt [162] electrodes in solid oxide fuel cells has enhanced rWGS rates, likely supporting the claim of the formate route. Nevertheless, steady-state isotopic transient kinetic analysis (SSITKA) combined with diffuse reflectance FT-IR spectroscopy (DRIFTS), revealed that the main intermediate species are carbonates, although the reaction could also take place through minor formates and carbonyls intermediates [110] (Figure 7). CO₂ adsorption as carbonates has also been observed on solid-liquid interfaces in the boundaries of a Pt/Al₂O₃ system [111].

There is, however, some agreement on the importance of the oxygen vacancies in the support. CO₂ is believed to adsorb on a ceria vacancy [108, 110] near a platinum/ceria boundary [110] or a platinum step [165]. Goguet et al. [110] have proposed that after CO₂ dissociative chemisorption (to CO and O_a), one O_a re-fills a vacancy and either CO is desorbed, or it can migrate to the Pt surface and desorb from there [110] where the amount of CO₂ decomposition depends on the oxidation state of the local CeO₂ interface [108]. Even in solid-liquid interfaces on Pt island film deposited on a Al₂O₃ film, the mechanism for rWGS is suspected to involve an O adatom (formed from CO₂ dissociation), which can refill an Al₂O₃ surface vacancy or recombine with adsorbed H [111].

The redox mechanism has been proved by Kim et al. on Pt/TiO₂ [139] and it is suspected to follow mostly a carbonate route, as described by Goguet et al. [110] on oxygen mobile supports. On the contrary, on non-reductive supports (i.e. Al₂O₃), the carbonyl route is suspected to occur [140]. The observation of different spectator species under different reaction conditions suggests that the forward and backwards WGS mechanism could be different (Pt/ceria) [112].

5c. Role of support

Primarily, the role of support effects on the rWGS mechanism has been focused on oxygen conduction materials such as ceria and perovskite-type oxides. The Au/CeO₂ system was proven more active than the Au/TiO₂ due to the higher oxygen mobility of ceria [166] and its ability to be re-oxidized by CO₂ [140]. This oxygen exchange can take place simultaneously (as in rWGS) or subsequently (as in rWGS-CL) [166]. In₂O₃ has been shown promising for CO₂ hydrogenation [145, 167]. On In₂O₃–CeO₂ catalysts, a volcano-type relationship between oxygen vacancies formation (increasing CeO₂) and reactive sites (increasing In₂O₃) was demonstrated [62]. When the ratio of oxides was 1:1 the activity of the rWGS was maximized and no side products were observed [62]. CO₂ can dissociate on the oxygen vacancies of ceria and on the Ni surface in a Ni/CeO₂ catalytic system [142]. The H₂ in the reaction would form more oxygen vacancies on the ceria, but its reduction is suspected to be catalyzed by Ni [142], similar to the mechanism on Pt/CeO₂ systems [140].

We have studied re-oxidation of pre-reduced La_{0.75}Sr_{0.25}CoO₃ (Figure 8) and found that the reactivity of the oxidant was O₂>H₂O>CO₂. Given the prior results from Wang et al., which suggest that the nature of the oxygen deposited on the reduced ceria surface is similar, whether it came from CO₂ or O₂ re-oxidation [166], our results suggest that dissociation of CO₂ is the rate determining step, and not the Oa migration or H₂ dissociation, in agreement with [58].

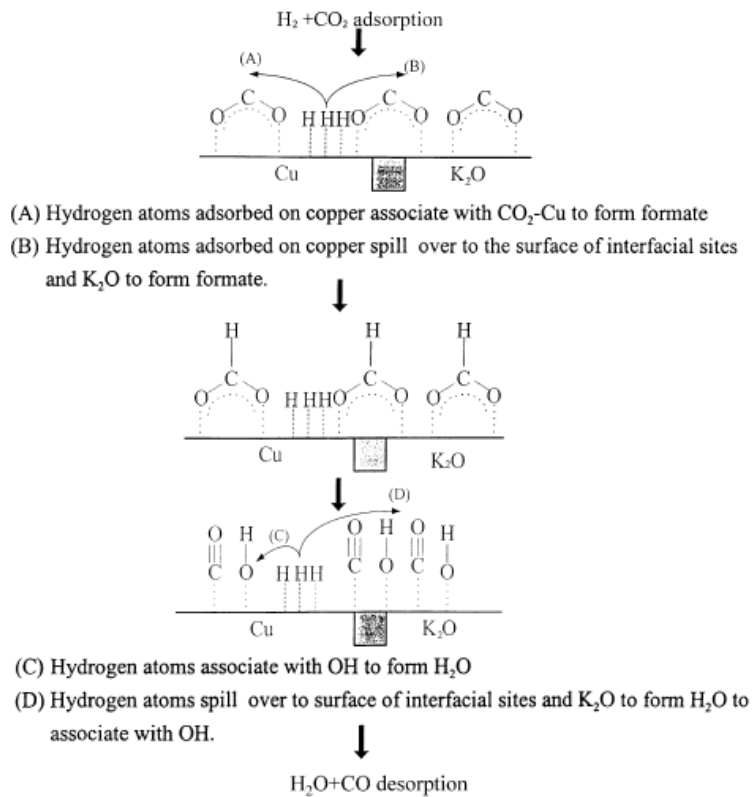


Figure 6. Proposed rWGS mechanism on the Cu/K/SiO₂ interface. Reproduced with permission from Elsevier (from [100]).

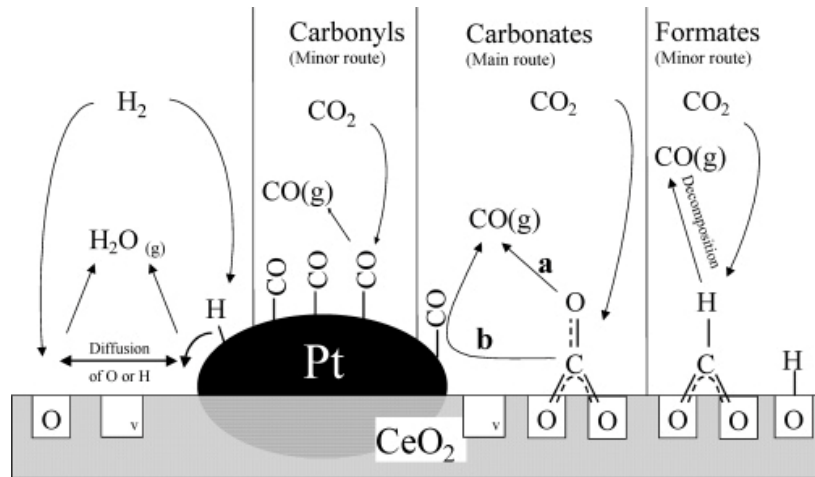


Figure 7. Proposed rWGS mechanism on the Pt/CeO₂ interface. Reproduced with permission from American Chemical Society (from [110]).

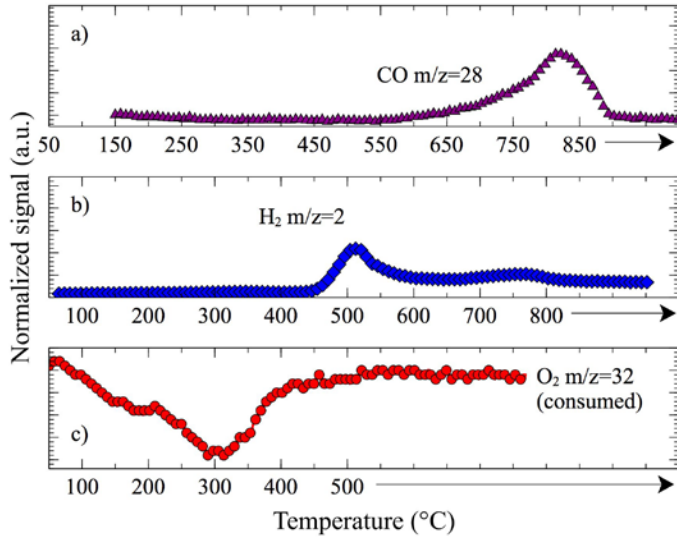


Figure 8. Oxidation of $\text{La}_{0.75}\text{Sr}_{0.25}\text{CoO}_3$ previously reduced with 10% H_2/He at $600\text{ }^\circ\text{C}$ for 30 min (total flow rate 50 sccm). a) Oxidation with CO_2 forming CO . b) Oxidation with H_2O forming H_2 . c) Consumption of O_2 .

7. Material selection and design principles

A fair and thorough comparison of catalysts is cumbersome because experimental conditions vary widely and, in a substantial number of cases, complete information is not reported (i.e. missing rates, conversions or yields). Supported platinum has achieved higher conversion than supported copper at $500\text{ }^\circ\text{C}$ [61]. But Cu-based catalyst are generally preferred due to their lower cost, high metal abundance and because Pt is highly susceptible to CO poisoning and coke formation [113]. The poisoning effect has also been observed on Pt and Ru/Pt alloy electrodes on PEMFCs [114]. Amongst the supports, ceria has been shown to play a key role on the reaction due to its high oxygen mobility [108, 110, 166]. Furthermore, catalytic research is progressing into a material design approach, so that control of metal and support surface faceting, and support vacancy amounts and locations for tuning surface properties is probably on the horizon for rWGS catalysis.

In addition, combining Cu and ceria components seems a natural idea. Cu supported on ceria has been previously studied for CO oxidation [168, 169] but recently, Rodriguez et al. have shown higher selectivity towards rWGS (vs. methanol or methane formation) on ceria supported on Cu surfaces [170] and Cu deposited on ceria and titania [171]. Therefore, it would likely be advantageous to thoroughly study Cu/ceria systems for the rWGS.

8. Summary and outlook

The rWGS is a promising reaction with high potential use in the near future for the large-scale conversion of CO_2 to CO , provided that a technology for production of renewable H_2 in large scale is also available. The rWGS reaction also requires lower temperatures ($\sim 200\text{ }^\circ\text{C}$ lower) than other conversion technologies that could meet CO_2 emissions scale. Being only slightly endothermic, the current challenge for rWGS use in fuel synthesis lies on designing materials that can achieve

high CO selectivity and production rates. Intensification strategies have recently been proposed to circumvent thermodynamic and kinetic limitations by using chemical looping to perform stoichiometric reactions rather than catalytic ones. Even though a large number of materials have been studied for the reaction, improvement is still possible. Some reports are often missing key information that allows for an equitable comparison and the effect of non-concentrated CO₂ has not been studied. Furthermore, if the rWGS reaction was to play a major role on atmospheric CO₂ concentration reduction, catalyst with earth abundant materials would be preferred.

In the interest of adopting earth abundant metals, iron oxides could be a good substitute for ceria. Fe oxides are also known to have high oxygen mobility and stability, and when added to a Cu system, have increased the rWGS activity [60, 96]. In a system where Cu particles would be supported on an iron oxide, Cu would provide high activity for CO formation whereas the Fe oxide would ideally bring high stability and high CO₂ adsorption [105]. MoC and CoMoC materials are also of interest due to their lack of precious metals and the convenience of employing industrially used metals.

Acknowledgments

The authors would like to acknowledge NSF award 1335817 for financial support. YAD acknowledges the Florida Education Fund for the McKnight Dissertation Fellowship and the NASA Florida Space Grant Consortium for the Dissertation Improvement Fellowship.

Table 2. Rates of CO production and CO₂ conversion on different materials.

Reference	Year	Material	T (°C)	P (bar)	Feed H ₂ /CO ₂ (v/v)	CO ₂ conversion (%)	CO Selectivity (%)	CO formation (μmol CO/g_cat/s)
Inoue et al. [117]	1989	Rh/TiO ₂	300	10.13	1/1			0.82
		Rh-Na/TiO ₂	260					0.43
		Rh/Nb ₂ O ₅	220					0.0
		Rh-Na/Nb ₂ O ₅	200					0.05
		Rh/MgO	200		3/1			0.008
		Rh/Nb ₂ O ₅	200					0.078
		Rh/ZrO ₂	200					0.033
		Rh/TiO ₂	300					0.93
Pettigrew et al. [140]	1994	Pd/Al ₂ O ₃	260	1	1/1		78 ^a	0.035 (μmol CO ₂ /g_cat/s)
		Pd/La ₂ O ₃ /Al ₂ O ₃					70	0.027
		Pd/PrO ₂ /Al ₂ O ₃					76	0.033
		Pd/CeO ₂ (5)/Al ₂ O ₃					87	0.045
		Pd/CeO ₂ (10)/Al ₂ O ₃					81	0.073
Ginés et al. [59]	1997	Commercial CuO/ZnO/Al ₂ O ₃	250	1	PH ₂ O / PCO ₂ O = 6	0.17		4.31
Bando et al. [120]	1998	Li/RhY (Li:Rh = 0)	250	30	3/1	24.1	0.3	
		Li/RhY (Li:Rh = 3)				12.0	3.7	
		Li/RhY (Li:Rh = 7)				11.1	27.6	
		Li/RhY (Li:Rh = 10)				13.1	86.6	
Chen et al. [101]	2000	10 wt% Cu/Al ₂ O ₃	500	1	1/9	60		9.0

Chen et al. [96]	2001	10%Cu–0.3%Fe/SiO ₂ w/w	600	1	1/1	12		
Kusama et al. [119]	2001	1 wt% Rh/SiO ₂	200	50	3/1	52	88.1	
Chen et al. [100]	2003	9% Cu/SiO ₂ w/w	600	1	1/1	5.3		
		9% Cu-1.9% K/SiO ₂ w/w				12.8		
Chen et al. [60]	2004	0.3% Fe/SiO ₂	600	1	1/1	1		
		10% Cu/SiO ₂				2		
		Cu-Fe/SiO ₂ (Cu/Fe = 10:0.3)				15		
		Cu-Fe/SiO ₂ (Cu/Fe = 10:0.8)				16		
Goguet et al [110]	2004	2%Pt/CeO ₂ by Johnson Matthey	225		4/1	13.7		2.2x10 ⁻⁴ mol CO/g
Dorner et al. [141]	2010	Mn 12 wt% / Fe 17 wt% / Al ₂ O ₃	290	13.8	3/1	37.7	10.7 (% CO yield)	
		Ce 2 wt% / Mn 12 wt% / Fe 17 wt% / Al ₂ O ₃				38.6	11.5 (% CO yield)	
		Ce 10 wt% / Mn 12 wt% / Fe 17 wt% / Al ₂ O ₃				35.8	17.5 (% CO yield)	
Gogate et al. [132]	2010	2% Rh/TiO ₂	270	20.26	1/1	7.89	14.5	
		2% Rh - 2.5% Fe / TiO ₂				9.16	28.4	
		2.5% Fe /TiO ₂				2.65	73.0	
Kim et al. [139]	2012	1% Pt/ Al ₂ O ₃	875		30/21	42		0.0104 s ⁻¹ (TOF at 300 °C)
		1% Pt/ TiO ₂				48		0.0998 s ⁻¹ (TOF at 300 °C)

Kim et al. [137]	2012	Pt/TiO ₂ (G) ^b	300			15		6480
Kharaji et al. [130]	2013	Fe/Al ₂ O ₃	600	10	1/1		35 (% CO yield)	96.17
		Mo/Al ₂ O ₃					33 (% CO yield)	80.14
		Fe-Mo/Al ₂ O ₃					37 (% CO yield)	128.2
Lu et al. [126]	2013	NiO/SBA-15	400	1	1/1	5	100	
			900			55	100	
Wang et al. [64]	2013	Ni-CeO ₂	750	1	1/1	40	100	
Lu et al. [122]	2014	(1 wt% NiO/CeO ₂) / 50% wt SBA-15	750 ^c	1	1/1	40	100	10.0 min ⁻¹ (TOF at ~90 °C)
		(3 wt% NiO/CeO ₂) / 50% wt SBA-15				45	100	4.5 min ⁻¹ (TOF at ~90 °C)
Kim et al. [150]	2014	BaZr _{0.8} Y _{0.2} O ₃	600		1/1	26.7	93	
		BaZr _{0.8} Y _{0.16} Zn _{0.04} O ₃				37.5	97	
		BaCe _{0.2} Zr _{0.6} Y _{0.16} Zn _{0.04} O ₃				36.3	94	
		BaCe _{0.3} Zr _{0.3} Y _{0.16} Zn _{0.04} O ₃				22.3	92	
		BaCe _{0.7} Zr _{0.1} Y _{0.16} Zn _{0.04} O ₃				10.8	74	
Oshima et al. [35] ^d	2014	10% mol La-ZrO ₂	150		1/1	18	100	
		1% wt Pt/10% mol La-ZrO ₂				40	99.5	
		1% wt Pd/10% mol La-ZrO ₂				30	98.2	
		1% wt Ni/10% mol La-ZrO ₂				28	96.5	
		1% wt Fe/10% mol La-ZrO ₂				28	100	
		1% wt Cu/10% mol La-ZrO ₂				28	100	

Porosoff et al. [133]	2014	PtCo/CeO ₂	300.85	1	2/1	6.6	4.5 (CO:CH ₄ ratio)	14.6 min ⁻¹ (TOF)
		PdNi/CeO ₂				2.5	0.6	5.6 min ⁻¹
		Mo ₂ C				8.7	14.5	25.7 min ⁻¹
		7.5 wt% Co/Mo ₂ C				9.5	51.3	16.1 min ⁻¹
		Unsupported Fe-oxide NPs				38	>85	
Xu et al. [134]	2015	β-Mo ₂ C	200	20	5/1	6	39	
		Cu/β-Mo ₂ C				4	44	
		Ni/β-Mo ₂ C				8	37	
		Co/β-Mo ₂ C				9	31	
Matsubu et al. [118]	2015	0.5% w/w Rh/TiO ₂	200		1/10			3.0 x 10 ⁻² CO molecule/Rh atoms/s (TOF)
		2% w/w Rh/TiO ₂						0.8
		4% w/w Rh/TiO ₂						0.4
		6% w/w Rh/TiO ₂						0.2
		In ₂ O ₃				16		
Wang et al. [62]	2016	In ₂ O ₃ :CeO ₂ = 3:1 w/w	500		1/1	17		
		In ₂ O ₃ :CeO ₂ = 1:1 w/w				20		
		In ₂ O ₃ :CeO ₂ = 1:3 w/w				11		
		In ₂ O ₃ :CeO ₂ = 1:9 w/w				9		
		CeO ₂				2.5		
This work	2016	La _{0.75} Sr _{0.25} FeO ₃	550	1	1/1	15.5	95	36.4

^aCalculated as: 100 - Methane selectivity. ^b For meaning of G (related to origin of the support) see reference [137]. ^c Non steady state.

^d Applying 3.0 mA input current.

Table 3. Proposed rate expressions

Ref.	Catalyst	Expression	Assumption
Kaiser et al. [17]	11% Ni / Al ₁₂ O ₁₉	$r_{m,pore} = \eta k_{m,CO_2} \left[C_{CO_2} - \frac{C_{CO} C_{H_2O} C_{H_2}^{-1}}{K_C} \right]$ $r_{m,ext} = \beta A_{m,ext} (C_{CO_2} - C_{CO,eq})$ $r_{m,eff} = \left[\frac{1}{r_{m,pore}} + \frac{1}{r_{m,ext}} \right]^{-1}$	Adiabatic. Only accurate for external or internal mass transport occurs, in-between regimes are approximations
Ginés et al. [59]	CuO/ZnO/Al ₂ O ₃	$r = \frac{k_1 L_0 P_{CO_2}^0 \left[P_{H_2}^0 (1-X)^2 - \frac{P_{CO_2}^0 X^2}{K} \right]}{P_{H_2}^0 (1-X) + \sqrt{K_2} P_{H_2}^0 1.5(1-X)^{1.5} + \frac{P_{CO_2}^0 X}{K_2 K_3}}$	CO ₂ dissociation is the rate-determining step. Rate deduced from Langmuir-Hinshelwood kinetics
Chen et al. [106]	ALE-Cu/SiO ₂	$r = 2^{1/2} k_4 K_1^{1/2} K_2^{1/2} K_3 P_{H_2}^{1/2} P_{CO_2}^{1/2}$	HCOO-2S → CO-S + OH-S is rate limiting ^a
Kim et al. [139] ^b	Pt/TiO ₂ and Pt/Al ₂ O ₃	$r = \frac{k_A k_B C_t (P_{CO_2} P_{H_2} - P_{CO} P_{H_2O} / K_{eq})}{(k_A P_{CO_2} + k_A P_{CO} + k_B P_{H_2} + k_B P_{H_2O})}$	The adsorption of CO and H ₂ O was excluded and the dissociation/adsorption step was excluded at low H ₂ pressure, 1 < P _{H₂} ⁰ / P _{CO₂} < 4

^a and other mathematical assumptions

^b Redox mechanism and associative mechanism

References

- [1] International Energy Agency, 2015 Key World Energy Statistics, Supply, Consumption and Emissions, 2015, Available at <https://www.iea.org/publications/freepublications/publication/key-world-energy-statistics-2015.html>
- [2] U.S. Department of Energy Office of Science, U.S. DOE, Carbon Cycling and Biosequestration: Integrating Biology and Climate Through Systems Science; Report from the March 2008 Workshop, 2008, Available at <http://genomicscience.energy.gov/carboncycle/report/index.shtml>
- [3] J.-B. Sallee, R.J. Matear, S.R. Rintoul, A. Lenton, *Nature Geosci* 5 (2012) 579.
- [4] C. Hauri, T. Friedrich, A. Timmermann, *Nature Clim. Change* 6 (2016) 172.
- [5] Global C.C.S. Institute, The Global Status of CCS: 2015, Summary Report, 2015, Available at <http://status.globalccsinstitute.com/>
- [6] G.C.C.S. Institute, Last access date February 17, 2016, Last updated 2015, <http://www.globalccsinstitute.com/projects/large-scale-ccs-projects>
- [7] M. Aresta, A. Dibenedetto, *Dalton Trans.* (2007) 2975.
- [8] M. Mikkelsen, M. Jorgensen, F.C. Krebs, *Energy Environ. Sci.* 3 (2010)
- [9] J.J. Dooley, R.T. Dahowski, C.L. Davidson, PNNL-17389 (2008)
- [10] R. Angamuthu, P. Byers, M. Lutz, A.L. Spek, E. Bouwman, *Science* 327 (2010) 313.
- [11] S. Sato, T. Arai, T. Morikawa, K. Uemura, T.M. Suzuki, H. Tanaka, T. Kajino, *J. Am. Chem. Soc.* 133 (2011) 15240.
- [12] G.A. Olah, A. Goeppert, G.K.S. Prakash, *J. Org. Chem.* 74 (2009) 487.
- [13] A. Goeppert, M. Czaun, J.-P. Jones, G.K. Surya Prakash, G.A. Olah, *Chem. Soc. Rev.* 43 (2014) 7995.
- [14] G. Job, S.D. Allen, C. Simoneau, R. Valente, J.J. Farmer, Metal complexes, Google Patents, USA, 2015.
- [15] P.E.A.o.P. Manufacturers, Plastics - the Facts 2015, Brussels, Belgium, 2015, pp. 1.
- [16] P.M. Mortensen, I. Dybkjær, *Appl. Catal. A: Gen.* 495 (2015) 141.
- [17] P. Kaiser, R.B. Unde, C. Kern, A. Jess, *Chem-Ing-Tech* 85 (2013) 489.
- [18] Department for Business, Innovation & Skills (BIS) and Department of Energy & Climate Change (DECC), E.E. Ltd, C.C. Ltd, P.S.E.P. Ltd, I. College, U.o. Sheffield, Demonstrating CO₂ capture in the UK cement, chemicals, iron and steel and oil refining sectors by 2025: A Techno-economic Study, Techno-economics of ICCS and CCU in UK, 2014, Available at <https://www.gov.uk/government/publications/co2-capture-in-the-uk-cement-chemicals-iron-steel-and-oil-refining-sectors>
- [19] X. Xiaoding, J.A. Moulijn, *Energy Fuels* 10 (1996) 305.
- [20] M.B. Ansari, S.-E. Park, *Energy Environ. Sci.* 5 (2012) 9419.
- [21] M. Poliakoff, W. Leitner, E.S. Streng, *Faraday Discuss.* 183 (2015) 9.
- [22] M. Institute, Last access date Last updated <http://www.methanol.org/Methanol-Basics.aspx>
- [23] I.E. Agency, Last access date 02/22/2016, Last updated 02/09/2016, <https://www.iea.org/oilmarketreport/omrpublic/>
- [24] U.S.E.I.A., Last access date 02/22/2016, Last updated 11/05/2015, http://www.eia.gov/Energyexplained/index.cfm?page=oil_refining
- [25] International Energy Agency, 2013 Key World Energy Statistics, Transformation, 2013, Available at http://www.iea.org/publications/freepublications/publication/KeyWorld2013_FINAL_WEB.pdf

[26] International Energy Agency, 2014 Key World Energy Statistics, Emissions, 2014, Available at <http://www.iea.org/publications/freepublications/publication/key-world-energy-statistics-2014.html>

[27] G. Centi, S. Perathoner, *Catal. Today* 148 (2009) 191.

[28] S. Chunshan, CO₂ Conversion and Utilization: An Overview, CO₂ Conversion and Utilization, American Chemical Society2002, pp. 2.

[29] T. Riedel, M. Claeys, H. Schulz, G. Schaub, S.-S. Nam, K.-W. Jun, M.-J. Choi, G. Kishan, K.-W. Lee, *Appl. Catal. A: Gen.* 186 (1999) 201.

[30] G. Centi, S. Perathoner, G. Iaquaniello, Realizing Resource and Energy Efficiency in Chemical Industry by Using CO₂, in: M. De Falco, G. Iaquaniello, G. Centi (Eds.) CO₂: A Valuable Source of Carbon, Springer London2013, pp. 27.

[31] S. Chu, A. Majumdar, *Nature* 488 (2012) 294.

[32] C. Song, *Catal. Tod.* 115 (2006) 2.

[33] O.-S. Joo, K.-D. Jung, I. Moon, A.Y. Rozovskii, G.I. Lin, S.-H. Han, S.-J. Uhm, *Ind. Eng. Chem. Res.* 38 (1999) 1808.

[34] N. Meiri, Y. Dinburg, M. Amoyal, V. Koukoulev, R.V. Nehemya, M.V. Landau, M. Herskowitz, *Faraday Discuss.* 183 (2015) 197.

[35] K. Oshima, T. Shinagawa, Y. Nogami, R. Manabe, S. Ogo, Y. Sekine, *Catal. Tod.* 232 (2014) 27.

[36] W. Wang, S. Wang, X. Ma, J. Gong, *Chem. Soc. Rev.* 40 (2011) 3703.

[37] E.V. Kondratenko, G. Mul, J. Baltrusaitis, G.O. Larrazábal, J. Pérez-Ramírez, *Energy Environ. Sci.* 6 (2013) 3112.

[38] International Renewable Energy Agency, IRENA, Renewable Energy Cost Analysis, Concentrating Solar Power, 2012, Available at <http://www.irena.org/menu/index.aspx?mnu=Subcat&PriMenuID=36&CatID=141&SubcatID=233>

[39] J.A. Turner, *Science* 305 (2004) 972.

[40] A. Hauch, S.D. Ebbesen, S.H. Jensen, M. Mogensen, *J. Mater. Chem.* 18 (2008) 2331.

[41] J. Kim, C.A. Henao, T.A. Johnson, D.E. Dedrick, J.E. Miller, E.B. Stechel, C.T. Maravelias, *Energy Environ. Sci.* 4 (2011) 3122.

[42] J. Kim, T.A. Johnson, J.E. Miller, E.B. Stechel, C.T. Maravelias, *Energy Environ. Sci.* 5 (2012) 8417.

[43] A. Taheri, E.J. Thompson, J.C. Fettinger, L.A. Berben, *ACS Catal.* 5 (2015) 7140.

[44] U.S. E.P.A., Global Anthropogenic Non-CO₂ Greenhouse Gas Emissions: 1990 - 2030, in: O.o.A.P.C.C. Division (Ed.), U.S. Environmental Protection Agency, Washington, DC, 2012.

[45] N.H. Elsayed, N.R.M. Roberts, B. Joseph, J.N. Kuhn, *Appl. Catal. B: Environ.* 179 (2015) 213.

[46] J. Skrzypek, M. Lachowska, D. Serafin, *Chem. Eng. Sci.* 45 (1990) 89.

[47] Q. Zhai, S. Xie, W. Fan, Q. Zhang, Y. Wang, W. Deng, Y. Wang, *Angew. Chem. Int. Ed.* 52 (2013) 5776.

[48] H. Zhou, J. Guo, P. Li, T. Fan, D. Zhang, J. Ye, *Sci. Rep.* 3 (2013)

[49] F.G. Acién Fernández, C.V. González-López, J.M. Fernández Sevilla, E. Molina Grima, *Appl. Microbiol. Biotechnol.* 96 (2012) 577.

[50] L. Gustavsson, P. Börjesson, B. Johansson, P. Svenningsson, *Energy* 20 (1995) 1097.

[51] K. Gao, K.R. McKinley, *J. Appl. Phycol.* 6 45.

[52] W.C. Chueh, C. Falter, M. Abbott, D. Scipio, P. Furley, S.M. Haile, A. Steinfeld, *Science* 330 (2010) 1797.

[53] P. Furler, J.R. Scheffe, M. Gorbar, L. Moes, U. Vogt, A. Steinfeld, *Energy Fuels* 26 (2012) 7051.

[54] J.E. Miller, M.D. Allendorf, R.B. Diver, L.R. Evans, N.P. Siegel, J.N. Stuecker, *J. Mater. Sci.* 43 (2008)

[55] A. Le Gal, S. Abanades, G. Flamant, *Energy Fuels* 25 (2011) 4836.

[56] A.H. McDaniel, E.C. Miller, D. Arifin, A. Ambrosini, E.N. Coker, R. O'Hayre, W.C. Chueh, *J. Tong, Energy Environ. Sci.* 6 (2013) 2024.

[57] A.H. Bork, M. Kubicek, M. Struzik, J.L.M. Rupp, *J. Mater. Chem. A* 3 (2015) 15546.

[58] K.-H. Ernst, C.T. Campbell, G. Moretti, *J. Catal.* 134 (1992) 66.

[59] M.J.L. Ginés, A.J. Marchi, C.R. Apesteguía, *Appl. Catal. A: Gen.* 154 (1997) 155.

[60] C.-S. Chen, W.-H. Cheng, S.-S. Lin, *Appl. Catal. A: Gen.* 257 (2004) 97.

[61] C.-S. Chen, J.H. Lin, J.H. You, C.R. Chen, *J. Am. Chem. Soc.* 128 (2006) 15950.

[62] W. Wang, Y. Zhang, Z. Wang, J.-M. Yan, Q. Ge, C.-J. Liu, *Catal. Tod.* 259 (2016) 402.

[63] B. Zhao, Y.-X. Pan, C.-J. Liu, *Catal. Tod.* 194 (2012) 60.

[64] L. Wang, H. Liu, Y. Liu, Y. Chen, S. Yang, *J. Rare Earth* 31 (2013) 969.

[65] P. Panagiotopoulou, D.I. Kondarides, X.E. Verykios, *Catal. Tod.* 181 (2012)

[66] K.-W. Jun, H.-S. Roh, K.-S. Kim, J.-S. Ryu, K.-W. Lee, *Appl. Catal. A: Gen.* 259 (2004) 221.

[67] C. Bosch, W. Wild, *Producing hydrogen*, Google Patents, 1914.

[68] D.S. Mallapragada, N.R. Singh, V. Curteanu, R. Agrawal, *Ind. Eng. Chem. Res.* 52 (2013) 5136.

[69] J.E. Whitlow, C.F. Parrish, *AIP Conference Proceedings* 654 (2003)

[70] D.P. VanderWiel, J.L. Zilka, Y. Wang, A.Y. Tonkovich, R.S. Wegeng, *Carbon Dioxide Conversions in Microreactors, IMRET 4: Proceedings of the 4th International Conference on Microreaction Technology, Topical Conference Proceedings, AIChE Spring National Meeting*; American Institute of Chemical EngineersAtlanta, GA, 2000, pp. 187.

[71] M.D. Porosoff, B. Yan, J.G. Chen, *Energy Environ. Sci.* 9 (2016) 62.

[72] P. Lanzafame, G. Centi, S. Perathoner, *Chem. Soc. Rev.* 43 (2014) 7562.

[73] G. Centi, E.A. Quadrelli, S. Perathoner, *Energy Environ. Sci.* 6 (2013) 1711.

[74] W. Wang, S. Wang, X. Ma, J. Gong, 40 (2011) 3703.

[75] W. Wang, J. Gong, *Front. Chem. Sci. Eng.* 5 (2011) 2.

[76] T. Sakakura, J.-C. Choi, H. Yasuda, *Chem. Rev.* 107 (2007) 2365.

[77] N.P. Siegel, J.E. Miller, I. Ermanoski, R.B. Diver, E.B. Stechel, *Ind. Eng. Chem. Res.* 52 (2013) 3276.

[78] G.P. Smestad, A. Steinfeld, *Ind. Eng. Chem. Res.* 51 (2012) 11828.

[79] T. Kodama, N. Gokon, *Chem. Rev.* 107 (2007) 4048.

[80] J.R. Rostrup-Nielsen, J. Sehested, *Adv. Catal.* 47 (2002) 65.

[81] M.C.J. Bradford, M.A. Vannice, *Catal. Rev. - Sci. Eng.* 41 (1999) 1.

[82] D. Pakhare, J.J. Spivey, *Chem. Soc. Rev.* 43 (2014) 7813.

[83] V. Havran, M.P. Dudukovi, C.S. Lo, *Ind. Eng. Chem. Res.* 50 (2011) 7089.

[84] E.V. Kondratenko, G. Mul, J. Baltrusaitis, G.O. Larrazabal, J. Perez-Ramirez, *Energy Environ. Sci.* 6 (2013) 3112.

[85] S.N. Habisreutinger, L. Schmidt-Mende, J.K. Stolarczyk, *Angew. Chem. Int. Ed.* 52 (2013) 7372.

[86] B. Kumar, M. Llorente, J. Froehlich, T. Dang, A. Sathrum, C.P. Kubiak, *Annu. Rev. Phys. Chem.* 63 (2012) 541.

[87] S.C. Roy, O.K. Varghese, P. Paulose, C.A. Grimes, *ACS Nano* (2010) 1259.

[88] V.P. Indrakanti, J.D. Kubicki, H.H. Schobert, *Energy Environ. Sci.* 2 (2009) 745.

[89] A.M. Appel, J.E. Bercaw, A.B. Bocarsly, H. Dobbek, D.L. DuBois, M. Dupuis, J.G. Ferry, E. Fujita, R. Hille, P.J.A. Kenis, C.A. Kerfeld, R.H. Morris, C.H.F. Peden, A.R. Portis, S.W. Ragsdale, T.B. Rauchfuss, J.N.H. Reek, L.C. Seefeldt, R.K. Thauer, G.L. Waldrop, *Chem. Rev.* 113 (2013) 6621.

[90] H. Arakawa, M. Aresta, J.N. Armor, M.A. Bartea, E.J. Beckman, A.T. Bell, J.E. Bercaw, C. Creutz, E. Dinjus, D.A. Dixon, K. Domen, D.L. DuBois, J. Eckert, E. Fujita, D.H. Gibson, W.A. Goddard, D.W. Goodman, J. Keller, G.J. Kubas, H.H. Kung, J.E. Lyons, L.E. Manzer, T.J. Marks, K. Morokuma, K.M. Nicholas, R. Periana, L. Que, J. Rostrup-Nielson, W.M.H. Sachtler, L.D. Schmidt, A. Sen, G.A. Somorjai, P.C. Stair, B.R. Stults, W. Tumas, *Chem. Rev.* 101 (2001) 953.

[91] N. von der Assen, P. Voll, M. Peters, A. Bardow, *Chem. Soc. Rev.* 43 (2014) 7982.

[92] L.-S. Fan, L. Zeng, W. Wang, S. Luo, *Energy Environ. Sci.* 5 (2012) 7254.

[93] N. MacDowell, N. Florin, A. Buchard, J. Hallett, A. Galindo, G. Jackson, C.S. Adjiman, C.K. Williams, N. Shah, P. Fennell, *Energy Environ. Sci.* 3 (2010) 1645.

[94] G. Goeppert, M. Czaun, G.K.S. Prakash, G.A. Olah, *Energy Environ. Sci.* 5 (2012) 7833.

[95] C. Ratnasamy, J.P. Wagner, *Catal. Rev.* 51 (2009) 325.

[96] C.-S. Chen, W.-H. Cheng, S.-S. Lin, *Chem. Commun.* (2001) 1770.

[97] S. Bebelis, H. Karasali, C.G. Vayenas, *Solid State Ionics* 179 (2008) 1391.

[98] S.-I. Fujita, M. Usui, N. Takezawa, *J. Catal.* 134 (1992) 220.

[99] J.A. Rodriguez, J. Evans, L. Feria, A.B. Vidal, P. Liu, K. Nakamura, F. Illas, *J. Catal.* 307 (2013) 162.

[100] C.-S. Chen, W.-H. Cheng, S.-S. Lin, *Appl. Catal. A: Gen.* 238 (2003) 55.

[101] C.-S. Chen, W.-H. Cheng, S.-S. Lin, *Catal. Lett.* 68 (2000) 45.

[102] J. Nakamura, J.A. Rodriguez, C.T. Campbell, *J. Phys.: Condens. Matter* 1 (1989) Sb149.

[103] C. Liu, T.R. Cundari, A.K. Wilson, *J. Phys. Chem. C* 116 (2012) 5681.

[104] S.-G. Wang, X.-Y. Liao, D.-B. Cao, C.-F. Huo, Y.-W. Li, J. Wang, H. Jiao, *J. Phys. Chem. C* 111 (2007) 16934.

[105] T. Bligaard, J.K. Nørskov, S. Dahl, J. Matthiesen, C.H. Christensen, J. Sehested, *J. Catal.* 224 (2004) 206.

[106] C.-S. Chen, J.H. Wu, T.W. Lai, *J. Phys. Chem. C* 114 (2010) 15021.

[107] C.-S. Chen, W.-H. Cheng, *Catal. Lett.* 83 (2002) 121.

[108] T. Jin, Y. Zhou, G.J. Mains, J.M. White, *J. Phys. Chem.* 91 (1987)

[109] D. Tibiletti, A. Goguet, F. Meunier, J.P. Breen, R. Burch, *Chem. Commun.* (2004) 1636.

[110] A. Goguet, F.C. Meunier, D. Tibiletti, J.P. Breen, R. Burch, *J. Phys. Chem. B* 108 (2004) 20240.

[111] D. Ferri, T. Bürgi, A. Baiker, *Phys. Chem. Chem. Phys.* 4 (2002) 2667.

[112] G. Jacobs, B.H. Davis, *Appl. Catal. A: Gen.* 284 (2005) 31.

[113] A. Goguet, F. Meunier, J.P. Breen, R. Burch, M.I. Petch, A.F. Ghenciu, *J. Catal.* 226 (2004) 382.

[114] T. Gu, W.-K. Lee, J.W. Van Zee, *Appl. Catal. B: Environ.* 56 (2005) 43.

[115] S. Alayoglu, S.K. Beaumont, F. Zheng, V.V. Pushkarev, H. Zheng, V. Iablokov, Z. Liu, J. Guo, N. Kruse, G.A. Somorjai, *Top. Catal.* 54 (2011) 778.

[116] P.G. Jessop, F. Joó, C.-C. Tai, *Coord. Chem. Rev.* 248 (2004) 2425.

[117] T. Inoue, T. Iizuka, K. Tanabe, *Appl. Catal.* 46 (1989) 1.

[118] J.C. Matsubu, V.N. Yang, P. Christopher, *J. Am. Chem. Soc.* 137 (2015) 3076.

[119] H. Kusama, K.K. Bando, K. Okabe, H. Arakawa, *Appl. Catal. A: Gen.* 205 (2001) 285.

[120] K.K. Bando, K. Soga, K. Kunimori, H. Arakawa, *Appl. Catal. A: Gen.* 175 (1998) 67.

[121] Y. Liu, D. Liu, *Int. J. Hydrogen Energ.* 24 (1999) 351.

[122] B. Lu, K. Kawamoto, *Mater. Res. Bull.* 53 (2014) 70.

[123] F.-M. Sun, C.-F. Yan, Z.-D. Wang, C.-Q. Guo, S.-L. Huang, *Int. J. Hydrogen Energy* 40 (2015) 15985.

[124] L. Wang, S. Zhang, Y. Liu, *J. Rare Earth* 26 (2008) 66.

[125] L. Wang, H. Liu, Y. Liu, Y. Chen, S. Yang, *J. Rare Earth* 31 (2013) 559.

[126] B. Lu, K. Kawamoto, *J. Environ. Chem. Eng.* 1 (2013) 300.

[127] B. Lu, Y. Ju, T. Abe, K. Kawamoto, *Inorg. Chem. Front.* 2 (2015) 741.

[128] J. Ko, B.-K. Kim, J.W. Han, *J. Phys. Chem. C* 120 (2016) 3438.

[129] D.H. Kim, S.W. Han, H.S. Yoon, Y.D. Kim, *J. Ind. Eng. Chem.* 23 (2015) 67.

[130] A.G. Kharaji, A. Shariati, M.A. Takassi, *Chin. J. Chem. Eng.* 21 (2013) 1007.

[131] A.G. Kharaji, A. Shariati, M. Ostadi, *J. Nanosci. Nanotechnol.* 14 (2014) 6841.

[132] M.R. Gogate, R.J. Davis, *Catal. Comm.* 11 (2010) 901.

[133] M.D. Porosoff, X. Yang, A.J. Boscoboinik, J.G. Chen, *Angew. Chem. Int. Ed.* 126 (2014) 6823.

[134] W. Xu, P.J. Ramírez, D. Stacchiola, J.L. Brito, J.A. Rodriguez, *Catal. Lett.* 145 (2015) 1365.

[135] T. Umegaki, K. Kuratani, Y. Yamada, A. Ueda, N. Kuriyama, T. Kobayashi, Q. Xu, *J. Power Sources* 179 (2008) 566.

[136] J. Ye, Q. Ge, C.-J. Liu, *Chem. Eng. Sci.* 135 (2015) 193.

[137] S.S. Kim, H.H. Lee, S.C. Hong, *Appl. Catal. B: Environ.* 119-120 (2012) 100.

[138] H. Sakurai, A. Ueda, T. Kobayashi, M. Haruta, *Chem. Commun.* (1997)

[139] S.S. Kim, H.H. Lee, S.C. Hong, *Appl. Catal. A: Gen.* 423–424 (2012) 100.

[140] D.J. Pettigrew, D.L. Trimm, N.W. Cant, *Catal. Lett.* 28 (1994) 313.

[141] R.W. Dorner, D.R. Hardy, F.W. Williams, H.D. Willauer, *Catal. Comm.* 11 (2010) 816.

[142] Y. Liu, Z. Li, H. Xu, Y. Han, *Catal. Comm.* 76 (2016) 1.

[143] S.-W. Park, O.-S. Joo, K.-D. Jung, H. Kim, S.-H. Han, *Appl. Catal. A: Gen.* 211 (2001) 81.

[144] O.-S. Joo, K.-D. Jung, *Bull. Korean Chem. Soc.* 24 (2003) 86.

[145] J. Ye, C. Liu, Q. Ge, *J. Phys. Chem. C* 116 (2012) 7817.

[146] L. Jia, J. Gao, W. Fang, Q. Li, *J. Rare Earths* 28 (2010) 747.

[147] H. Zhan, F. Li, P. Gao, N. Zhao, F. Xiao, W. Wei, L. Zhong, Y. Sun, *J. Power Sources* 251 (2014) 113.

[148] L. Jia, J. Gao, W. Fang, Q. Li, *Catal. Comm.* 10 (2009) 2000.

[149] M.A. Ulla, R.A. Migone, J.O. Petunchi, E.A. Lombardo, *J. Catal.* 105 (1987) 107.

[150] D.H. Kim, J.L. Park, E.J. Park, Y.D. Kim, S. Uhm, *ACS Catal.* 4 (2014) 3117.

[151] Y.A. Daza, D. Maiti, R.A. Kent, V.R. Bhethanabotla, J.N. Kuhn, *Catal. Tod.* 258 (2015) 691.

[152] Y.A. Daza, R.A. Kent, M.M. Yung, J.N. Kuhn, *Ind. Eng. Chem. Res.* 53 (2014) 5828.

[153] Y.A. Daza, D. Maiti, B.J. Hare, V.R. Bhethanabotla, J.N. Kuhn, *Surf. Sci.* 648 (2016) 92.

[154] M. Najera, R. Solunke, T. Gardner, G. Veser, *Chem. Eng. Res. Des.* 89 (2011) 1533.

[155] R.D. Solunke, G. Veser, *Ind. Eng. Chem. Res.* 49 (2010) 11037.

[156] V.V. Galvita, H. Poelman, V. Bliznuk, C. Detavernier, G.B. Marin, *Ind. Eng. Chem. Res.* 52 (2013) 8416.

[157] N.V.R.A. Dharanipragada, L.C. Buelens, H. Poelman, E.D. Grave, V.V. Galvita, G.B. Marin, *J. Mater. Chem. A* 3 (2015) 16251.

[158] C. Nordhei, K. Mathisen, I. Bezverkhyy, D.G. Nicholson, *J. Phys. Chem.* 112 (2008)

[159] C. Nordhei, K. Mathisen, O. Safonova, W. van Beek, D.G. Nicholson, *J. Phys. Chem.* 113 (2009) 19568.

[160] D. Maiti, Y.A. Daza, M.M. Yung, J.N. Kuhn, V.R. Bhethanabotla, *J. Mater. Chem. A* 4 (2016) 5137.

[161] C.T. Campbell, K.-H. Ernst, Forward and Reverse Water-Gas Shift Reactions on Model Copper Catalysts, *Surface Science of Catalysis*, American Chemical Society 1992, pp. 130.

[162] G. Pekridis, K. Kalimeri, N. Kaklidis, E. Vakouftsi, E.F. Iliopoulos, C. Athanasiou, G.E. Marnellos, *Catal. Tod.* 127 (2007) 337.

[163] G. Karagiannakis, S. Zisekas, M. Stoukides, *Solid State Ionics* 162-163 (2003) 313.

[164] F. Solymosi, *J. Mol. Catal.* 65 (1991) 337.

[165] J. Xu, J.T. Yates Jr, *Surf. Sci.* 327 (1995)

[166] L.C. Wang, M. Tahvildar Khazaneh, D. Widmann, R.J. Behm, *J. Catal.* 302 (2013) 20.

[167] Q. Sun, J. Ye, C.-J. Liu, Q. Ge, *Greenhouse Gas. Sci. Technol.* 4 (2014)

[168] D. Gamarra, G. Munuera, A.B. Hungría, M. Fernández-García, J.C. Conesa, P.A. Midgley, X.Q. Wang, J.C. Hanson, J.A. Rodríguez, A. Martínez-Arias, *J. Phys. Chem. C* 111 (2007) 11026.

[169] N. E. Nunez, H. P. Bideberripe, M. L. Casella, G. J. Siri, *Current Catalysis* 3 (2014) 187.

[170] J.A. Rodriguez, P. Liu, D.J. Stacchiola, S.D. Senanayake, M.G. White, J.G. Chen, *ACS Catal.* 5 (2015) 6696.

[171] J. Graciani, K. Mudiyanselage, F. Xu, A.E. Baber, J. Evans, S.D. Senanayake, D.J. Stacchiola, P. Liu, J. Hrbek, J. Fernández-Sanz, J.A. Rodriguez, *Science* 345 (2014) 546.